Lasers in Medical Science
https://doi.org/10.1007/s10103-021-03308-y

ORIGINAL ARTICLE

Photobiomodulation combined with adipose-derived stem cells encapsulated in methacrylated gelatin hydrogels enhances in vivo bone regeneration

Mert Calis[1] · Gülseren Irmak[2,3] · Tugrul Tolga Demirtaş[2,4] · Murat Kara[1] · Galip Gencay Üstün[1] · Menemşe Gümüşderelioğlu[2,5] · Ayten Türkkanı[6] · Ayşe Nur Çakar[6] · Figen Özgür[1]

Received: 24 November 2020 / Accepted: 28 March 2021

Abstract

Reconstruction of bone defects is still a significant challenge. The aim of this study was to evaluate the effect of application of photobiomodulation (PBM) to enhance in vivo bone regeneration and osteogenic differentiation potential of adipose-derived stem cells (ADSCs) encapsulated in methacrylated gelatin (GEL-MA) hydrogels. Thirty-six Sprague-Dawley rats were randomly separated into 3 experimental groups ($n = 12$ each). The groups were control/blank defect (I), GEL-MA hydrogel (II), and ADSC-loaded GEL-MA (GEL-MA+ADSC) hydrogel (III). Biparietal critical sized bone defects (6 mm in size) are created in each animal. Half of the animals from each group ($n = 6$ each) were randomly selected for PBM application using polychromatic light in the near infrared region, 600–1200 nm. PBM was administered from 10 cm distance cranially in 48 h interval. The calvaria were harvested at the 20th week, and macroscopic, microtomographic, and histologic evaluation were performed for further analysis. Microtomographic evaluation demonstrated the highest result for mineralized matrix formation (MMF) in group III. PBM receiving samples of group III showed mean MMF of 79.93±3.41%, whereas the non-PBM receiving samples revealed mean MMF of 60.62±6.34 % (p=0.002). In terms of histologic evaluation of bone defect repair, the higher scores were obtained in the groups II and III when compared to the control group (2.0 for both PBM receiving and non-receiving specimens; p<0.001). ADSC-loaded microwave-induced GEL-MA hydrogels and periodic application of photobiomodulation with polychromatic light appear to have beneficial effect on bone regeneration and can stimulate ADSCs for osteogenic differentiation.

Keywords Polychromatic light · Microwave-induced methacrylated gelatin · Adipose-derived stem cells · Calvarial defect · Bone regeneration

Introduction

Reconstruction of bone defects is still a significant challenge of plastic surgery [1]. Current modalities for achieving this goal such as autologous bone grafting [2], microvascular transfer of vascularized bone flaps, and using distraction osteogenesis [3] all have limitations and certain complications. From this standpoint, recent advances in bone tissue engineering aiming to offer a readily available bone construct with ideal biocompatibility have been the center of attention in regenerative medicine [4].

The three-dimensional (3D) hydrogel is an especially encouraging material due to its hydrophilic nature and its capability to ensure biomimetic environments with tunable mechanical and biological properties for supporting the development of new bone tissue within the bioengineered tissue constructs [5]. Injectable hydrogels could cover in defect size and

✉ Mert Calis
mertcalis@gmail.com

1 Department of Plastic Reconstructive and Aesthetic Surgery, Faculty of Medicine, Hacettepe University, Ankara, Turkey

2 Department of Bioengineering, Faculty of Engineering, Hacettepe University, Ankara, Turkey

3 Department of Bioengineering, Faculty of Engineering and Nature Sciences, Malatya Turgut Ozal University, Malatya, Turkey

4 Department of Basic Pharmaceutical Sciences, Faculty of Pharmacy, Erciyes University, Kayseri, Turkey

5 Department of Chemical Engineering, Faculty of Engineering, Hacettepe University, Ankara, Turkey

6 Department of Histology and Embryology, School of Medicine, TOBB University, Ankara, Turkey

Published online: 11 April 2021

suitably coalesce with the main tissue; therefore, they are capable and useful materials for tissue engineering [6]. Gelatin is derived from collagen and has a nearly same fundamental molecular unit of collagen [7]. However, it is necessary to develop bioactive gelatin by functionalization with acrylic groups. Methacrylated gelatin (GEL-MA) is formed by chemical bonding of methacrylate groups and the amine-containing side groups of gelatin. GEL-MA can be chemically crosslinked with the addition of a photoinitiator by UV [8]. In our group, it was previously reported that microwave-induced methacrylated gelatin (Mw-GEL-MA) enhanced stiffness and degradation of gelatin and also supported in vitro bone tissue formation. In addition, GEL-MA and its modified forms, which can be photo-crosslinked, have also been used for bioprinting systems [9].

Light energy was initially used by Mester [10] for regenerative purposes by application of low-level laser therapy (LLLT) and had been in use for various purposes for more than 40 years [11]. Currently, many variations of laser therapies have evolved and "photobiomodulation" (PBM) became the general term used to define the use of related light sources such as incoherent light (light-emitting diodes—LED) or coherent light (laser) sources for regenerative purposes [12, 13]. On the cellular level, PBM is well known to stimulate the mitochondrial respiratory chain reactions [14], increase the synthesis of ATP [15], and increase the intracellular production of nitric oxide and therefore activates angiogenetic pathways and increases wound healing on tissue level [16]. Overall effects of PBM are stimulation of collagen synthesis [17], cell proliferation [17, 18], cell differentiation [17, 19, 20], and platelet activation [15]. This effect depends on the type of source of used and the wavelength applied for the low-level light therapies. Even though the regenerative effect of PBM has been observed in several studies, the effect of application of PBM as polychromatic light in the near infrared region on the differentiation of ADSCs is still uncertain [21, 22].

Recently, application of polychromatic light in wider spectrum including near infrared (NIR) wavelengths is proposed for optimal benefit [23]. In this study, we applied a combined strategy using therapeutic cells (ADSCs) encapsulated biomimetic Mw-GEL-MA hydrogel and polychromatic light in the NIR to improve in situ bone regeneration and observe osteogenic differentiation of ADSCs.

Materials and methods

Synthesis of methacrylated gelatin and formation of GEL-MA hydrogels

GEL-MA was synthesized via the microwave-induced methacrylation reaction according to previous report of our group [9]. Briefly, type A gelatin solution (10%, w/v) was obtained dissolving it in phosphate-buffered saline (PBS, pH: 7.4) at 50 °C. Reaction was realized into a microwave synthesis device (Milestone, Italy) at 50−60 °C. Methacrylic anhydride (4%, v/v) was injected at the ratio of 0.4 mL/min to the solution by a syringe pump. Microwave irradiation was used for 5 min at 1000 W power. For the purifying of Gel-MA, at the end of the reaction, the Gel-MA solution was transferred to dialysis membrane and dialyzed against deionized water for 1 day at 40 °C. Then, the purified product was freeze dried. The degree of methacrylation (DM) was determined as 90% via ^{1}H-NMR spectroscopy in deuterium oxide at 40 °C [9]. For animal experiments, GEL-MA (15%, w/v) was dissolved in Irgacure (photo initiator) solution (0.3%, v/v). GEL-MA hydrogel solution (pH 7.0) was slowly injected (nozzle tip diameter 2 mm) to cranial defects at a volume of 50 μL. Immediately after the injection, hydrogels were crosslinked via a UV-A (300-500 nm, 200 mW/cm^2, Tanses Technologies, Canada) for 40 s.

SEM analysis and live-dead assay

Freeze dried and gold–palladium coated GEL-MA hydrogels were viewed via a scanning electron microscopy (SEM, Zeiss, Germany).

ADSC-loaded hydrogels were incubated in a growth medium of α-MEM with 15% (v/v) serum, 0.4% (v/v) penicillin-streptomycin, 0.2% v/v amphotericin B, and 0.2% v/v gentamicin in the CO_2 incubator at 37 °C. Live/dead analysis was performed on the 1st day of culture. The cell-loaded hydrogels were incubated in 2 μM Calcein AM and 4 μM ethidium homodimer (Ethd-1) solution for 30 min. After washing with PBS (pH 7.4), hydrogels were visualized via a confocal microscope (CLSM, Zeiss, LSM 510, Germany). Images taken from the top, middle, and bottom parts of the hydrogels were analyzed via ImageJ software, and cell viability (%) was calculated.

Preparation of adipose-derived mesenchymal stem cell–loaded GEL-MA hydrogels

ADSCs used in the study are obtained from the perirenal adipose fat pad of Sprague-Dawley rats. ADSC isolation protocol and characterization analysis in terms of confirmation of cells were done in a previous study by our group [24]. α-minimal essential medium enriched standard growth medium, 10% (v/v) fetal bovine serum (FBS), 0.1% (v/v) amphotericin B, and 1% (v/v) penicillin-streptomycin were used for expansion of ADSCs. Incubation conditions of the cells were 37 °C with 5% CO_2 (Heraus Instruments, Germany). Third passage ADSCs were used in this study. As described in "Synthesis of methacrylated gelatin and formation of GEL-MA hydrogels," sterile conditions were obtained for preparation of the GEL-

MA hydrogel solutions. ADSCs (1×10^6 cells/mL) were gently dispersed into sterile Gel-MA hydrogel solutions, and the temperature of the syringe was kept at 35–37 °C via the heating pad to minimize the shear stress that develops on the cells. ADSC-loaded GEL-MA hydrogel solutions were injected to defect as described in "Synthesis of methacrylated gelatin and formation of GEL-MA hydrogels" (Figs. 1a and 2a).

Labeling of adipose-derived mesenchymal stem cells with bromodeoxyuridine

Bromodeoxyuridine reagent (BrdU, Invitrogen Life Technologies, USA) is a thymidine analogue was used for labelling of ADSCs in vivo. Briefly, BrdU was diluted in 1:100 (v/v) with cell culture medium. Then, culture medium of ADSCs was changed with the diluted BrdU solution. The ADSCs were incubated in the diluted BrdU solution for 2 h at 37 °C.

Animal model and surgical procedure

Thirty-six non-immunosuppressed Sprague-Dawley rats (250 to 350 g) were used. All animals were fed ad libitum and kept in 12 h day/night cycle. The animals were kept at standardized temperature and humidity environment at Hacettepe University Animal Research Center.

Animals (36) were randomly separated into 3 experimental groups (n = 12 each). The groups were control/blank defect (I), methacrylated gelatin (GEL-MA) hydrogel (II), and ADSC-loaded GEL-MA (GEL-MA+ADMSC) hydrogel (III). Half of the animals from each group (n = 6 each) were randomly selected for polychromatic light application. These animals received PBM in 48 h interval for 20 weeks while the other half did not (Table 1).

Intraperitoneal administration of xylazine (12.5 mg/kg) and ketamine hydrochloride (87.5 mg/kg) mixture was used for induction of general anesthesia. Sterile conditions were obtained for the whole surgical procedure. After complete shaving the surgical site was prepped with povidone iodine antiseptic solution (Baticon; Drogsan, Turkey). V-shaped incision at the dorsum of the scalp was planned for access; lamination of the tissue planes was done for separate elevation of scalp flap and the periosteum. Dental burr was used for creation of symmetric two round critical sized bone defects at the parietal bones (6 mm in diameter) (Fig. 1a). Surgical approach was done delicately to keep dura mater was intact in all animals. Depending on the experimental group, ADSC-loaded GEL-MA hydrogel solution was injected to cranial defects at a volume of 50 μL via a micropipette (Eppendorf Research,

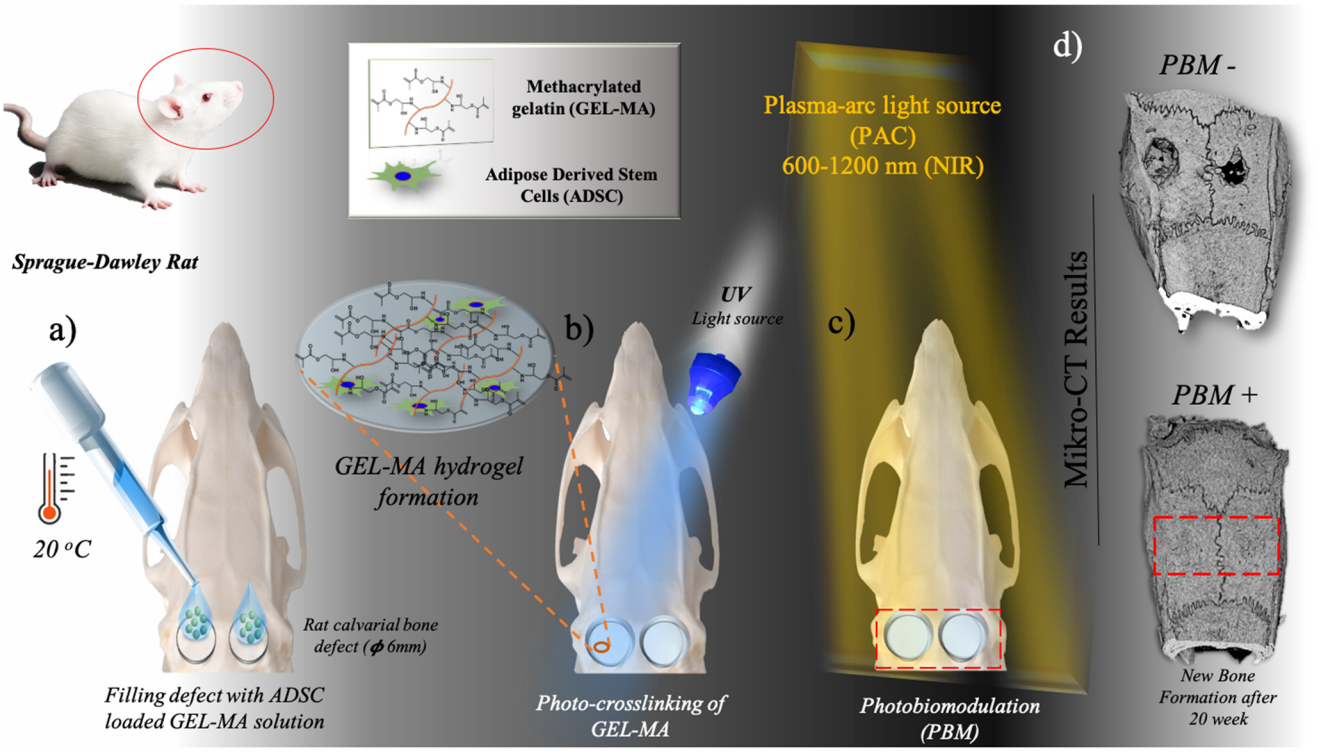

Fig. 1 Schematic diagrams of bone regeneration combined with ADSC-encapsulated GEL-MA hydrogels by photobiomodulation. **a** Filling rat calvarial defects with ADSC-loaded GEL-MA solution. **b** Photocrosslinking of GEL-MA solution with UV light source (300–500 nm). It is applied for 40 s to calvarial bone defects. **c** PBM is managed via a polychromatic light source (600- to 1200-nm wavelengths). Standard protocol involves application of PBM from 10 cm distance cranially in 48 h interval in animals receiving PBM. **d** Micro CT results of mineralized matrix formation. Control/blank defect (PBM-) and GEL-MA+ADSC hydrogel (PBM+), respectively

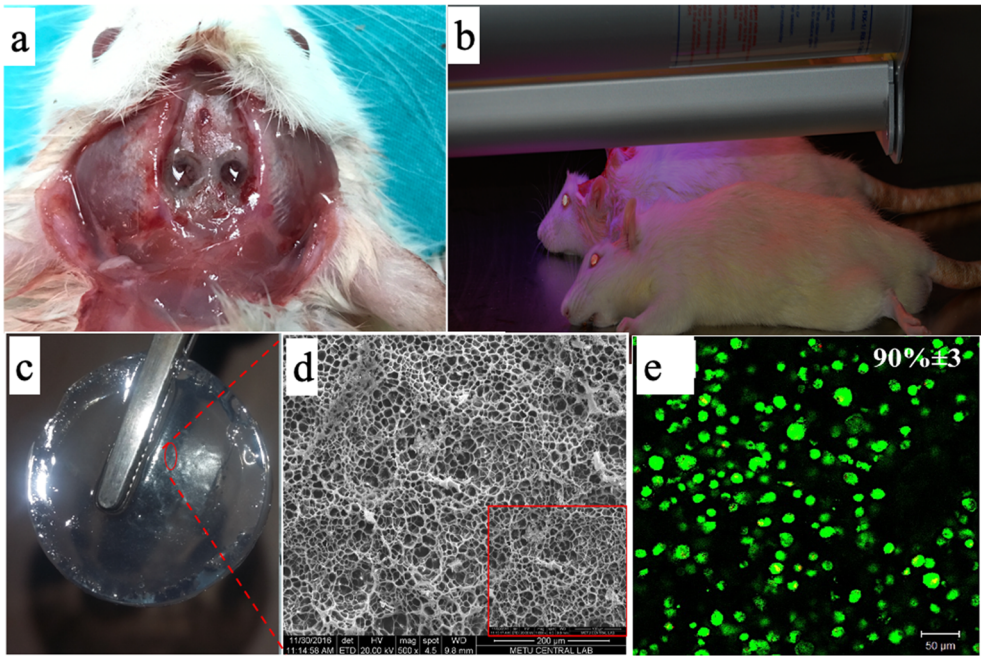

Fig. 2 **a** Biparietal critical sized calvarial bone defect. Note that the methacrylated hydrogel tissue scaffold is applied to both defects (50 μL). **b** Application of UV light for photocrosslinking. **c** Methacrylated hydrogel used in the study. **d** Scanning electron micrograph (SEM) images of microwave assisted methacrylated gelatin (GEL-MA) hydrogels ×500 magnification, inset; porous structure of hydrogel (×5000 magnification). **e** Live-dead assay: Illustrative fluorescent image of labeled ADSCs in the GEL-MA hydrogel on day 1 (scale bar 50 μm). Live cells appear in green, and dead is red

Sigma-Aldrich, Germany) (Fig. 2a) and UV light (300–500 nm) was applied for crosslinking of the hydrogel (Figs. 1b and 2b). Scalp flap was redraped and skin repair was done using absorbable sutures. Sacrification of the animals was done 20 weeks after surgery with overdose application of the previously mentioned general anesthetic mixture. The calvarium was harvested as a whole, and macroscopic, microtomographic, and histologic evaluations were performed for further analysis (Fig. 1d).

Application of polychromatic light

PBM is administered via a polychromatic light source (Collagentex RX-1, Collagentex®, Tanses Technologies, Montreal, Canada) which is able to provide light energy with 633-, 666-, 712-, 812- 1018-, and 1128-nm wavelengths. The device itself is able to block any emission below 600 nm and above 1200 nm. Specially doped quartz plasma arc lamp with a band pass filter and reflector system integrated to the device utilizes 685 W of power into 600- to 1200-nm wavelengths of visible light and infrared light. The light intensity from the outer acrylic shield at 20 cm distance is 2.6 J/cm^2 min. Our standard protocol involves application of PBM from 20 cm distance cranially for 10 min in each session. Thus, total dose received for single session of PBM application is 26 J/cm^2. Sessions are planned in 48 h intervals in animals receiving PBM through the experimental period (Fig. 1c). The first PBM application after surgical intervention took place under anesthesia, whereas the following PBM applications did not require anesthesia.

Table 1 Experimental groups of the study. The groups were control/blank defect (I), methacrylated gelatin (GEL-MA) hydrogel (II), and ADSC-loaded GEL-MA (GEL-MA+ADMSC) hydrogel (III). Half of the animals from each group (n = 6 each) were randomly selected for PBM application (GEL-MA: methacrylated gelatin hydrogel tissue scaffold, GEL-MA+ADSC: methacrylated gelatin hydrogel tissue scaffold loaded with adipose-derived mesenchymal stem cells, PBM: photobiomodulation, PBM-: non-PBM receiving, PBM+: PBM receiving, n: sample size)

Groups	PBM– (n)	PBM+ (n)	Total (n)
I. Control	6	6	12
II. GEL-MA	6	6	12
III. GEL-MA+ADSC	6	6	12

Microcomputerized tomography analysis

Whole calvarium specimens obtained with sacrification were placed in and kept in phosphate formalin solution (10%) for fixation. Compact X-ray microcomputerized tomography (microCT) device (Skyscan 1174; Bruker, Belgium) was used for imaging of the specimens. The raw data was reconstructed for obtaining 2D/3D images (Fig 1d). These reconstructed images were analyzed (Skyscan CT-analyzer; Bruker, Belgium) to calculate the percent of mineralized matrix formation (MMF) and the microporosity (MP) for both quantitative and qualitative analyses of bone formation in the area of interest.

Histological analysis

De Castro solution was used for decalcification of the calvarial bone samples. Protocol involves steps of fixation, dehydration

of bones in ethanol, clearance in xylene, and embedding in paraffin. Longitudinal sections of 5-μm thickness were obtained using a microtome (Leica Microsystems, Germany). The samples were stained with hematoxylin-eosin and Masson trichrome stains. ADSC containing samples were additionally immunohistochemically stained to trace the cells labeled with BrdU in vivo. A modified scoring system [25] was used for evaluation (Table 2).

Statistical analysis

Statistical analysis was done using SPSS for Windows 25.0 (Statistical Package for Social Sciences; IBM Corporation, USA). Shapiro-Wilk test was used for assessment of distribution, and the homogeneity of the variances was tested using Levene tests. For evaluation of the microtomographic analysis, independent samples *T* test was used, whereas for the evaluation of histological analysis, Mann-Whitney *U* test with Monte Carlo simulation was used. Post hoc analysis was made using the Fisher least significant difference (LSD) and the Dunn tests. Descriptive statistical values were expressed as medians ± interquartile range and the categorical values were expressed as n (%). *p* values less than 0.05 were considered as statistically significant.

Results

Hydrogel formation and characterization

At the first step of hydrogel formation, gelatin was methacrylated successfully (DM>90%) and rapidly (in 5 min) by microwave energy. Then, microwave-induced GEL-MA hydrogels was covalently crosslinked via application of UV light for 40 s and stable GEL-MA hydrogels were obtained (Fig. 2 a, b, and c). Microwave-induced GEL-MA hydrogels were characterized in terms of mechanical and biomimetic properties in a previous study by our group [9]. It was demonstrated that compression module of GEL-MA hydrogel is 60.3 ±9.0 kPa. Besides, in rheological studies, storage and loss modules were obtained as 41.1 and 0.1 kPa, respectively at frequency of 100 rad/s [9]. Also it was determined that GEL-MA hydrogels less degraded after 35 days in collagenase solution [9]. In this study, interconnected pore structure of GEL-MA hydrogels was confirmed by SEM and average pore diameters of the freeze-dried hydrogels were confirmed as 65 μm by using ImageJ (Fig. 2d). Fluorescent images showed that cells were homogeneously dispersed in hydrogel. ADSC viability was determined higher than 90% (Fig. 2e).

Results of in vivo study

Sacrification of the animals was done 20 weeks after surgery with overdose application of the previously mentioned general anesthetic mixture. The calvarium was harvested as a whole, and macroscopic, microtomographic, and histologic evaluations were performed for further analysis.

Macroscopic evaluation

Macroscopic evaluation of the control group revealed only granulation and showed no signs of total bone regeneration. Among all specimens none of them revealed signs of infection of foreign body reaction. Among the specimens of groups II and III (other than the control group), no obvious difference was observed with macroscopic view. The hydrogel scaffolds were not totally resorbed and were observed at the center of the defects at the end of the 20th week (Fig. 3a–f).

Microcomputerized tomography analysis

Two-dimensional images are further reconstructed to 3D images (Fig. 3a–f), and the samples are evaluated for mineralized matrix formation and microporosity in the bone defect areas (Table 3).

At the end of the 20th weeks, means of both MMF and MP for both PBM receiving and non-receiving samples of all groups demonstrated better healing than the control group ($p < 0.001$). For MMF, highest result was observed in group III (GEL-MA+ADSC). The non-PBM receiving samples of this group revealed mean MMF of 60.62±6.34%, whereas the PBM receiving samples showed mean MMF of 79.93 ±3.41% (p=0.002). Post hoc comparison of the groups II (GEL-MA) and III (GEL-MA+ADSC) revealed significant difference among the MMF results of PBM receiving samples

Table 2 Histological scoring system modified from previous studies of Bolgen et al. [25] was used in this study. This involves evaluation of new bone formation in the original defect and fibrous connective tissue formation in response to application of the experimental process

Parameter	Scores			
	0	1	2	3
New bone formation	None	Mild (<%50)	Moderate (>%50)	Full (100%)
Fibrous connective tissue formation	None	Mild to moderate formation	Moderate to dense formation	Dense formation

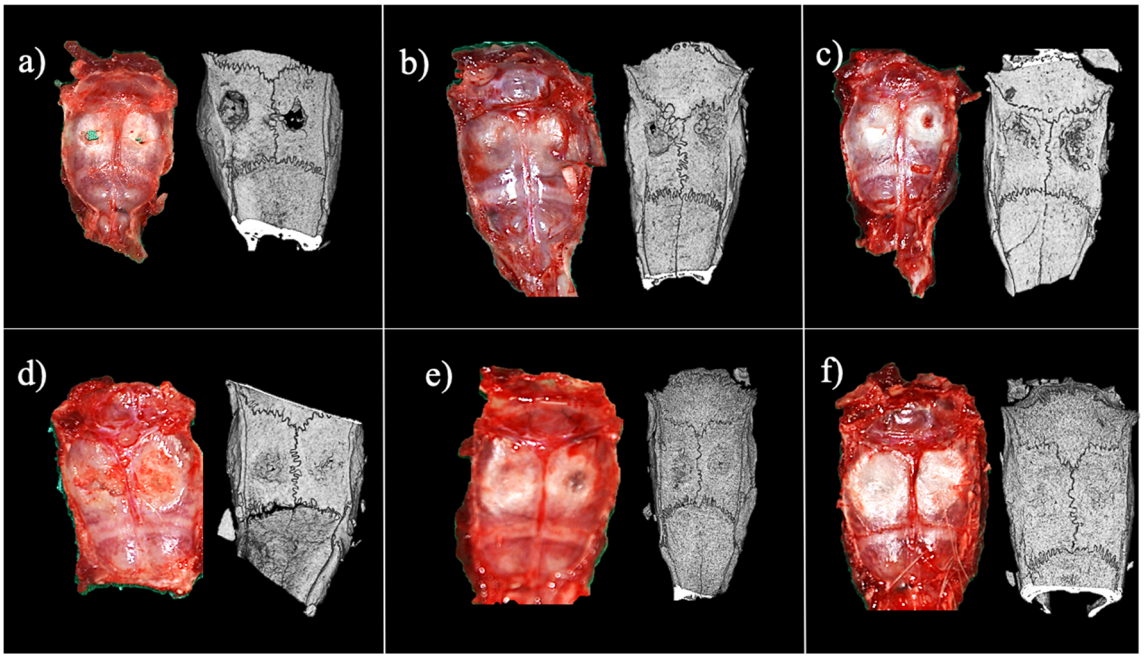

Fig. 3 Macroscopic appearances (left) and microtomographic images (right) of the specimens at the end of the 20th week demonstrating the bone healing at the end of the 20th week. **a** Control/defect (PBM-). **b** Methacrylated gelatin hydrogel (PBM-). **c** ADSC-loaded methacrylated gelatin hydrogel (PBM-). **d** Control/defect (PBM+). **e** Methacrylated gelatin hydrogel (PBM+). **f** ADSC-loaded methacrylated gelatin hydrogel (PBM+)

(p<0.001), whereas the results of non-PBM receiving samples were found to be comparable (p=0.237).

In means of MP, all groups demonstrated better healing than the control group (p < 0.001). Control group demonstrated the highest microporosity rates (71.74%±11.93 for non-PBM receiving, 69.18%±4.65 for PBM receiving samples), and the results were found to be comparable in means of PBM application (p=0.601). Post hoc comparison of the MP rates of PBM non-receiving samples of groups II and III were found to be comparable (p=0.238), whereas MP rates of PBM

Table 3 Results of microtomographic evaluation at the end of 20 weeks. At the end of the 20th weeks, means of both MMF and MP for both PBM receiving and non-receiving samples of all groups demonstrated better healing than the control group (p < 0.001). For MMF, highest result was observed in group III (GEL-MA+ADSC). Post hoc comparison of the groups II (GEL-MA) and III (GEL-MA+ADSC) revealed significant difference among the MMF results of PBM receiving samples (p<0.001), whereas the results of non-PBM receiving samples were found to be comparable (p=0.237). Post hoc comparison of the MP rates of PBM non-receiving samples of groups II and III was found to be comparable (p=0.238), whereas MP rates of PBM receiving samples of groups 3 were found to be significantly better than the results of group II (p<0.001)

	Microporosity %		p	Mineralized matrix formation %		p
	PBM- Mean±SD	PBM+ Mean±SD		PBM- Mean±SD	PBM+ Mean±SD	
GEL-MA+ADSC (A)	39.38±6.34	20.08±3.41	**0.002**[1]	60.62±6.34	79.93±3.41	**0.002**[1]
Gel-MA (B)	45.69±7.37	31.98±4.88	**0.008**[1]	54.30±7.35	68.02±4.88	**0.008**[1]
Control (C)	71.74±11.93	69.18±4.65	0.601[1]	28.60±11.94	30.82±4.65	0.643[1]
p value	**<0.001**[2]	**<0.001**[2]		**<0.001**[2]	**<0.001**[2]	
Pairwise comparison						
A→B	0.238	**<0.001**		0.237	**<0.001**	
A→C	**<0.001**	**<0.001**		**<0.001**	**<0.001**	
B→C	**<0.001**	**<0.001**		**<0.001**	**<0.001**	

SD standard deviation

[1] Independent samples *T* test (bootstrap)

[2] One-way ANOVA (Brown-Forsythe); post hoc test: Fisher's least significant difference (LSD)

Significant values are marked as bold for receiving attention

receiving samples of groups 3 were found to be significantly better than the results of group II ($p<0.001$).

Histological analysis

Histologic samples of groups I (control), II (GEL-MA), and III (GEL-MA+ADSC) are demonstrated depending on their PBM application in Figs. 4a–h and 5a–h. The control group, which only has critical sized bone defects, has a thin membrane of granulation tissue at the border of the filling the cavity and whether PBM received or not did not demonstrate new bone formation. The groups II and III demonstrated signs of new bone formation and demonstrated regular and irregular collagen reorganizations. At the end of 20 weeks, the remnants of GEL-MA hydrogel were still observable in the histologic specimens. Immunohistochemical staining shows the presence of BrdU-positive ADSCs at the periphery of hydrogel, in the zones of dense connective tissue, and new bone formation (Figs. 4g–h and 5g–h).

In order to further evaluate the samples at the end of the 20th weeks and compare the impact of PBM on healing profiles, a modified scoring system involving assessment of "bone defect repair" and "fibrous connective tissue formation" was used (Table 4).

In terms of bone defect repair, the highest scores were obtained in the groups II and III when compared to the control group (2.0 for both PBM receiving and non-receiving specimens; $p<0.001$). In respect to application of PBM, bone defect healing results of groups II and III were also found to be comparable ($p=0.542$ and $p=0.999$, respectively).

In means of fibrous connective tissue formation, the highest result was obtained in the group III (GEL-MA+ADSC), and it was significantly higher than the control group for both PBM receiving and non-receiving samples ($p<0.001$). The post hoc analysis revealed no significant difference between the results of groups II and III in means of PBM application ($p=0.403$ and $p=0.776$, respectively). On the other hand, post hoc analysis of stem cell loaded samples of group III demonstrated significantly better healing in PBM received samples when compared to the control group ($p=0.015$), whereas PBM received samples of group II did not ($p=0.570$).

Discussion

Bone tissue engineering, intending to provide readily available substitute for replacing tissue defects, has grown a great attention throughout the recent decades as current surgical reconstruction options such as autologous bone grafting, distraction osteogenesis, microvascular transfer of bone flaps, and composite tissue transplantation still have significant limitations and drawbacks [26–28].

Success in bone tissue engineering necessitates well appreciation of tissue healing and bone regeneration steps [29]. Ideal construct should meet the criteria of being osteoinductive as well as being osteoconductive [30]. From this standpoint, current approach focuses on the integration of cellular strategies [31, 32]. In the early of 2000s, Zuk et al. [33, 34] introduced adipose tissue as a reserve for mesenchymal stem cells and, with the discovery of ADSCs, many studies aiming to integrate these cells to tissue engineering strategies had been made. Besides their potential for tissue regeneration as stem cells can differentiate to various cells, osteogenic transformation has been the main topic of interest for bone tissue engineering strategies. Using special culture media, osteogenic transformation of ADSCs in vitro has been successfully achieved, whereas differentiation of ADSCs in vivo may need induction with special agents [35].

PBM is an adjunctive procedure used for accelerating regeneration for more than forty years. Initially, Mester [10, 36, 37] introduced photoenergy to have a beneficial effect on all phases of wound healing [38]. Later on, it is demonstrated that photons induce mitochondrial cytochrome c oxidase and induce series of respiratory chain reactions, which significantly increase intracellular levels of ATP, reactive oxygen species, and nitric oxide, leading to increased proliferation, epithelization, and angiogenesis [39, 40].

However, the application of PBM is not as simple as described. The modality of light source selected and the wavelength applied on the tissue are two major determinants of the regenerative outcome. Although application of PBM is expected to increase the regeneration [41], another light source carbon dioxide laser is used for nonsurgical debulking of flaps [42]. The spectrum of wavelength to be applied ranges from 390 to 1100 nm, and various effects on different tissues had been obtained. The light sources also varies being coherent and non-coherent and involves low-level laser devices, filtered lamps or light emitting diodes (LEDs). PBM is applied via relatively novel approach using a polychromic light source capable of applying light energy in extremely wide spectrum from 600 to 1200 nm.

The main aim of the study was to investigate the effect of polychromatic light applied in NIR and provide a baseline to compare the outcomes with conventional devices on bone regeneration and osteogenic induction of ADSCs. The critical-sized bone defect model, used in this study, is not expected to heal on its own and was initially described by Hollinger [43, 44]. For the reconstruction of the defect, GEL-MA hydrogel was used. GEL-MA is composed of chemical functionalization of methacrylic anhydride with type A gelatin [45, 46]. Gelatin, being obtained from denaturation of collagen, is a component of ECM and therefore it is highly osteoinductive [47, 48]. Functionalization with MA provides to photo-crosslinkable form to the gelatin, and it enables osteoconductivity for bone tissue engineering studies [8].

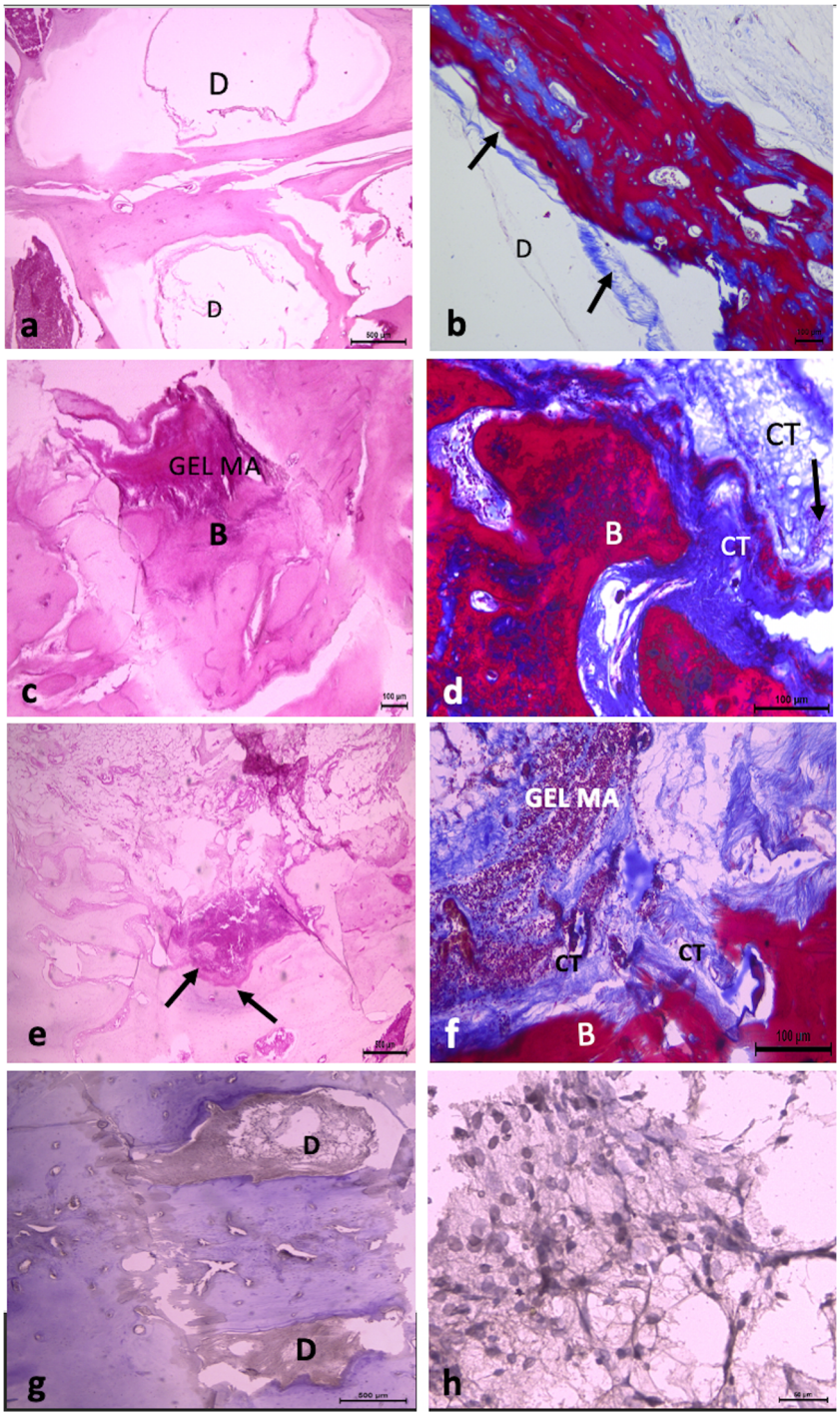

Fig. 4 Histological appearances of the non-PBM receiving (PBM-) specimens at the end of the 20th week. **a**, **b** Control group (PBM-). The defect cavities are not filled with granulation tissue. At the border of the bone, dense connective tissue has started to form indicating new bone formation (arrows). D, defect. **a** Hematoxylin-eosin staining ×4. **b** Masson trichrome stain ×10. **c**, **d** Methacrylated gelatin hydrogel (PBM-). The defect cavity is filled methacrylated gelatin hydrogel. Hydrogel filled cavities are surrounded by new bone formation (marked as B). Dense connective tissue (marked as CT) formation around the hydrogel filling the defect cavity. Hydrogel-filled cavities are surrounded by new bone formation (marked as B). **c** Hematoxylin-eosin ×10. **d** Masson trichrome ×20. **e**, **f** ADSC-loaded methacrylated gelatin hydrogel (PBM-). Dense connective tissue (marked as CT) almost fills the defect cavity around the hydrogel. New bone (marked as B, arrows) is developing around and in the hydrogel replacing as it degradates. **e** Hematoxylin-eosin. **e** ×4. **f** Masson trichrome ×20. **g**, **h** ADSC-loaded methacrylated gelatin hydrogel (PBM-). Both of the defect cavities are filled with dense connective tissue except the central region. Immunohistochemical staining confirms presence of BrdU-labeled stem cells in the central connective tissue formation zone. Anti-BrdU indirect immune peroxidase. **g** ×4. **h** ×40

Mw-induced methacrylated hydrogels is eligible for long-term regeneration studies because it enables ideal mechanical stability and biodegradation rate [9]. Microwave-induced methacrylated gelatin (Mw-GEL-MA) is firstly introduced with our study group [9]. It was proved that, in contrast to the limitations of the conventional methacrylation method, this approach provided rapid functionalization of the gelatin and leaded to higher degree of methacrylation. Besides, it was showed that Mw-GEL-MA hydrogels and their polymerization conditions are suitable in terms of cell viability and differentiation of pre-osteoblastic cells [9].

Analysis of the microtomographic evaluation revealed that significantly better mineralized matrix formation in both GEL-MA and GEL-MA+ADSC applied samples when compared to the control group. The highest rate of mineralized matrix formation was observed in the PBM applied GEL-MA+ADSC group. When the PBM application is taken in consideration, the PBM receiving samples demonstrated significantly better mineralized

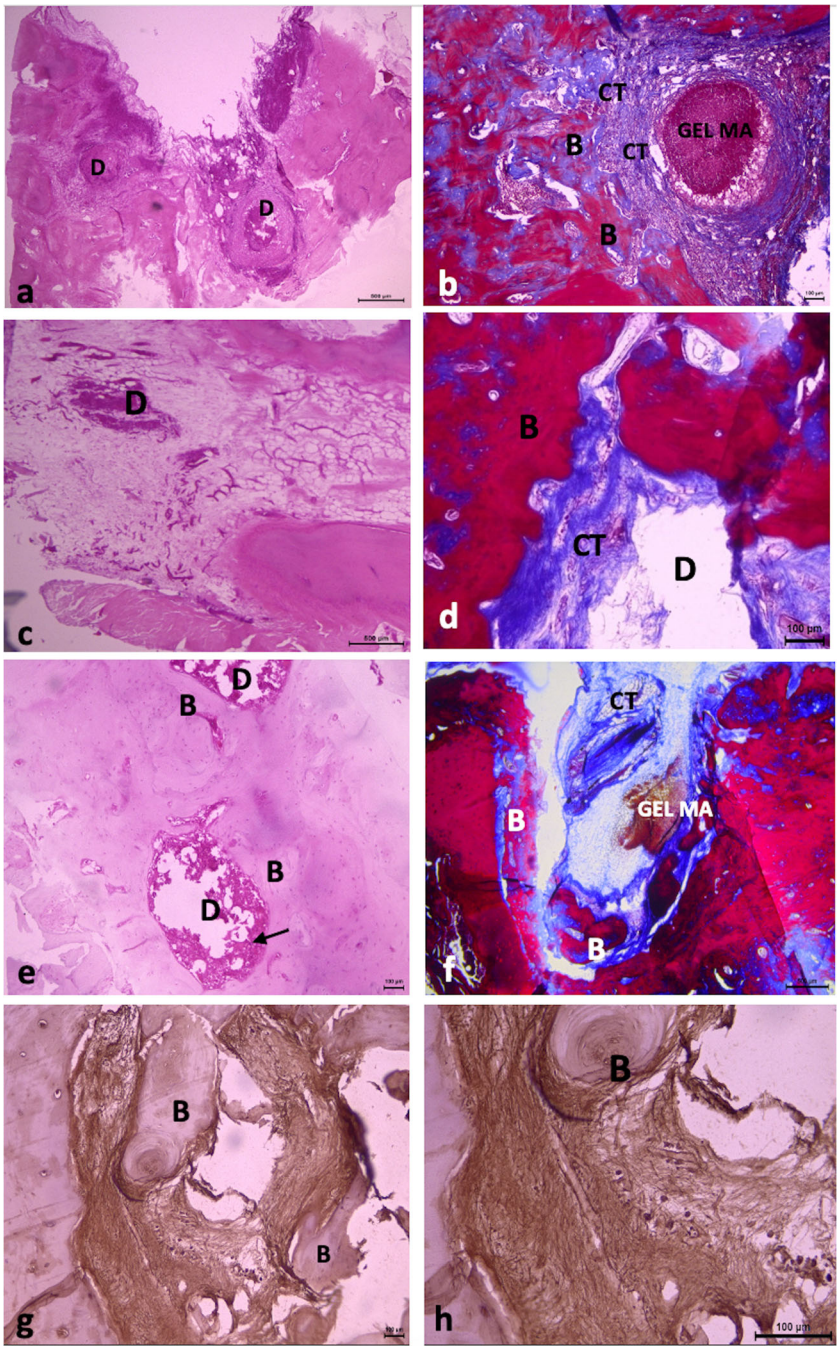

Fig. 5 Histological appearances of the PBM receiving (PBM+) specimens at the end of the 20th week. **a**, **b** Control group (PBM+). Both of the defect cavities (marked as D) are filled with granulation tissue and surrounded by dense connective tissue (marked as CT) and new bone formation (marked as B). **a** Hematoxylin-eosin ×4. **b** Masson trichrome ×10. **c**, **d** Methacrylated gelatin hydrogel (PBM+). Defect cavity (marked as D) is filled with methacrylated hydrogel. Vascular dense connective tissue (marked as CT) in the defect cavity is surrounded by new bone formation (marked as B) (marked as D). Defect cavity is filled with calcified and non-calcified bone spicules except the mid-region in another subject. **c** Hematoxylin-eosin ×4. **d**, **e** Masson trichrome. **d** ×10. **e**, **f** ADSC-loaded methacrylated gelatin hydrogel (PBM+). Both defect cavities (marked as D) are filled methacrylated hydrogel surrounded by new bone formation (marked as B). The cavity is filled with dense connective tissue (marked as CT). New bone (marked as B) spicules is present in the connective tissue. Newly formed membranous bone is observed around the defect adjacent to calcified bone. **e** Hematoxylin-eosin ×4. **f** Masson trichrome ×10. **g**, **h** ADSC-loaded methacrylated gelatin hydrogel (PBM+). Immunohistochemical staining demonstrates bromodeoxyuridine and adipose-derived mesenchymal stem cells around the remnants of tissue scaffold, at the site of new bone formation (marked as B), and dense connective tissue formation. Note the relative abundance of the BrdU-positive ADSCs at the PBM receiving group. Anti-BrdU indirect immune peroxidase. **g** ×4. **h** ×20

Table 4 Results of histologic evaluation at the end of 20 weeks. In terms of bone defect repair, the highest scores were obtained in the groups II and III when compared to the control group (2.0 for both PBM receiving and non-receiving specimens; $p<0.001$). In respect to application of PBM, bone defect healing results of groups II and III were also found to be comparable ($p=0.542$ and $p=0.999$, respectively). In means of fibrous connective tissue formation, the highest result was obtained in the group III (GEL-MA+ADSC), and it was significantly higher than the control group for both PBM receiving and non-receiving samples ($p<0.001$)

	New bone formation		*p*	Fibrous connective tissue formation		*p*
	PBM- Med. (min/max)	PBM+ Med. (min/max)		PBM- Med. (min/max)	PBM+ Med. (min/max)	
GEL-MA+ADSC (A)	2 (1/2)	2 (2/3)	0.542[1]	2 (2/2)	3 (2/3)	0.062[1]
Gel-MA (B)	2 (1/2)	2 (2/2)	0.999[1]	2 (1/2)	2.5 (2/3)	0.277[1]
Control (C)	0 (0/0)	0 (0/1)	0.458[1]	1 (1/1)	2 (1/2)	0.062[1]
p value	**<0.001[2]**	**<0.001[2]**		**0.002[2]**	**0.019[2]**	
Pairwise comparison						
A→B	0.999	0.999		0.776	0.403	
A→C	**0.003**	**0.001**		**0.001**	**0.015**	
B→C	**0.003**	**0.005**		**0.024**	0.570	

Med. median, *min* minimum, *Max* maximum

[1] Mann-Whitney *U* test(Monte Carlo)

[2] Kruskal-Wallis test (Monte Carlo); post hoc test: Dunn's test

Significant values are marked as bold for receiving attention

matrix and microporosity profiles. Interestingly, in the control group, PBM receiving and PBM non-receiving samples revealed comparable results.

Analysis of histologic evaluation demonstrated a thin membrane of dense connective granulation tissue in the control group and samples of this group did not show signs of bone healing. According to the standardized scoring system used in the study, in means of new bone formation and fibrous connective tissue formation, the GEL-MA and GEL-MA+ADSC groups revealed better healing results when compared to control group. Microscopic observations revealed better bone formation in ADSC containing groups especially in PBM receiving samples. Although the highest scores in means of new bone formation and fibrous connective tissue formation were observed in the GEL-MA+ADSC group, the pairwise comparison of groups with each other did not show significantly better results among the samples of GEL-MA and GEL-MA+ADSC groups. In contrast to the microtomographic evaluation, PBM receiving and PBM non-receiving samples demonstrated comparable results among all groups.

Determining the ideal time period for evaluation of late term bone healing in experimental studies depends on several factors. One of them is the biodegradation kinetics of the tissue scaffold. It is expected that the construct degradates as the tissue is healing, and the goal is the total replacement of the biomaterial as the regeneration takes place. Another leading determinant of bone healing is the regenerative capacity of the biological microenvironment. ADSCs are well known for their higher regenerative capacity and longer life span. In this study, the samples were obtained following intermittent application of PBM for overall duration of 20 weeks to investigate the late term effect of PBM on ADSCs. Total bone healing is not expected to be observed despite this long period due to the preference of critical-sized bone defect model of Hollinger [44]. The main outcome is reached depending on the comparison of the healing profiles of the experimental groups.

ADSCs being ubiquitous and easily accessed became of the most promising cell populations for regenerative purposes [49]. Subcutaneous adipose tissue from various sites such as abdomen, thigh, or arms is the best known and widely accepted donor sites for ADSC harvest, whereas there is growing interest for harvesting this cell population from visceral adipose cell sources [50]. Visceral adipose tissue is also known for high content of white adipose tissue which has relatively higher preference than brown adipose tissue for regenerative studies [51]. Recent studies demonstrated that adipose tissue located at different sites may have distinct cellular compositions and diverse biological behavior. Perirenal fat had been the source of the ADSCs used in the study, and there are not many studies focusing on the effect of visceral ADSCs compared to the stem cells harvested subcutaneously [52]. Like ADSCs harvested from subcutaneous anatomical areas, demonstrating in vivo osteogenic differentiation potential of perirenal ADSCs is also one of the striking features of this study.

Application of PBM in polychromatic fashion appears to have a beneficial effect on bone regeneration in bone defects reconstructed using GEL-MA and ADSC-loaded GEL-MA hydrogels. Methacrylated gelatin hydrogel used in this study revealed significant bone healing in both microtomographic and histologic evaluation when compared to control groups. Microwave-assisted synthesized GEL-MA appears to be a

suitable composite for in vivo tissue engineering studies. On the other hand, GEL-MA being still detectable at the end of 20 weeks displays a suboptimal biodegradation profile. Immunohistochemically, the presence of ADSCs around the remnants of the hydrogel in the zones of new bone formation in the PBM receiving samples supports the hypothesis that PBM may stimulate ADSCs for osteogenic differentiation.

Conclusion

This is a pioneer study for demonstrating the regenerative effect of photobiomodulation with polychromatic light in the NIR, and it is potential osteoinductive effect on adipose-derived mesenchymal stem cells in vivo. Further studies will clarify the intracellular mechanisms and side effect profile and lead to clinical translation of photobiomodulation for bone regeneration applications. Consequently, using ADSC-loaded microwave-induced GEL-MA hydrogels and periodic application of photobiomodulation with polychromatic light appears to have beneficial effect on bone regeneration and can stimulate ADSCs for osteogenic differentiation. On the other hand, ADSC-loaded GEL-MA hydrogel system may be used in situ bioprinting approach in which bone tissue is to be printed directly on the intended anatomical location in the living body.

Author contribution Mert Calis designed the animal study, conducted the experiments, and wrote the paper. Murat Kara and Galip Gencay Üstün contributed the animal experiments, postoperative care, and application of the PBM. Gülseren Irmak and Tuğrul Tolga Demirtaş prepared the stem cells and the biomaterials for the study. Tuğrul Tolga Demirtaş and Mert Calis performed the microCT analyses. Ayşe Nur Çakar and Ayten Türkkanı performed the histological analyses. Menemşe Gümüşderelioğlu and Figen Özgür designed and supervised the study and edited the final manuscript.

Funding This work was supported from the Hacettepe University Scientific Research Foundation (Grant No: THD-2017-14465).

Declarations

Ethical approval The study was conducted, and all animal experiments were performed following approval of the Institutional Review Board of Hacettepe University on Experimental Studies (Approval no.: 2017/29-04).

Conflict of interest The authors declare no competing interests.

References

1. Fearon JA, Griner D, Ditthakasem K, Herbert M (2017) Autogenous bone reconstruction of large secondary skull defects. Plast Reconstr Surg 139:427–438
2. Perry CR (1999) Bone repair techniques, bone graft, and bone graft substitutes. Clin Orthop Relat Res:71–86
3. McCarthy JG, Stelnicki EJ, Mehrara BJ, Longaker MT (2001) Distraction osteogenesis of the craniofacial skeleton. Plast Reconstr Surg 107:1812–1827
4. Roseti L, Parisi V, Petretta M, Cavallo C, Desando G, Bartolotti I, Grigolo B (2017) Scaffolds for bone tissue engineering: State of the art and new perspectives. Mater Sci Eng C Mater Biol Appl 78: 1246–1262
5. Zhang YS, Khademhosseini A (2017) Advances in engineering hydrogels. Science 356
6. Kim BS, Cho CS (2018) Injectable hydrogels for regenerative medicine. Tissue Eng Regen Med 15:511–512
7. Fang XX, Xie J, Zhong LX, Li JR, Rong DM, Li XS, Ouyang J (2016) Biomimetic gelatin methacrylamide hydrogel scaffolds for bone tissue engineering. J Mater Chem B 4:1070–1080
8. Van den Bulcke AI, Bogdanov B, De Rooze N, Schacht EH, Cornelissen M, Berghmans H (2000) Structural and rheological properties of methacrylamide modified gelatin hydrogels. Biomacromolecules 1:31–38
9. Irmak G, Demirtas TT, Gumusderelioglu M (2019) Highly methacrylated gelatin bioink for bone tissue engineering. Acs Biomater Sci Eng 5:831–845
10. Mester E, Spiry T, Szende B, Tota JG (1971) Effect of laser rays on wound healing. Am J Surg 122:532–535
11. Dodd EM, Winter MA, Hordinsky MK, Sadick NS, Farah RS (2018) Photobiomodulation therapy for androgenetic alopecia: a clinician's guide to home-use devices cleared by the Federal Drug Administration. J Cosmet Laser Ther 20:159–167
12. Hennessy M, Hamblin MR (2017) Photobiomodulation and the brain: a new paradigm. J Opt 19:013003
13. Kuffler DP (2016) Photobiomodulation in promoting wound healing: a review. Regen Med 11:107–122
14. Karu T (1989) Laser biostimulation: a photobiological phenomenon. J Photochem Photobiol B 3:638–640
15. Irmak G, Demirtaş TT, Gümüşderelioğlu M (2019) Sustained release of growth factor from photoactivated platelet rich plasma (PRP). Eur J Pharm Biopharm 2020 Mar 148:67–76
16. Gupta A, Avci P, Sadasivam M, Chandran R, Parizotto N, Vecchio D, de Melo WC, Dai T, Chiang LY, Hamblin MR (2013) Shining light on nanotechnology to help repair and regeneration. Biotechnol Adv 31:607–631
17. Ulker N, Cakmak AS, Kiremitci AS, Gumusderelioglu M (2016) Polychromatic light-induced osteogenic activity in 2D and 3D cultures. Lasers Med Sci 31:1665–1674
18. Soleimani M, Abbasnia E, Fathi M, Sahraei H, Fathi Y, Kaka G (2012) The effects of low-level laser irradiation on differentiation and proliferation of human bone marrow mesenchymal stem cells into neurons and osteoblasts-an in vitro study. Lasers Med Sci 27: 423–430
19. Cakmak AS, Cakmak S, Vatansever HS, Gumusderelioglu M (2018) Photostimulation of osteogenic differentiation on silk scaffolds by plasma arc light source. Lasers Med Sci 33:785–794. https://doi.org/10.1007/s10103-017-2414-4
20. El Nawam H, El Backly R, Zaky A, Abdallah A (2019) Low-level laser therapy affects dentinogenesis and angiogenesis of in vitro 3D cultures of dentin-pulp complex. Lasers Med Sci 34:1689–1698
21. Lin F, Josephs SF, Alexandrescu DT, Ramos F, Bogin V, Gammill V, Dasanu CA, De Necochea-Campion R, Patel AN, Carrier E, Koos DR (2010) Lasers, stem cells, and COPD. J Transl Med 8:16
22. Oliveira FA, Matos AA, Santesso MR, Tokuhara CK, Leite AL, Bagnato VS, Machado MA, Peres-Buzalaf C, Oliveira RC (2016) Low intensity lasers differently induce primary human osteoblast proliferation and differentiation. J Photochem Photobiol B 163: 14–21

23. Calis M, Demirtas TT, Sert G, Irmak G, Gumusderelioglu M, Turkkani A, Cakar AN, Ozgur F (2019) Photobiomodulation with polychromatic light increases zone 4 survival of transverse rectus abdominis musculocutaneous flap. Lasers Surg Med 51:538–549
24. Akdere OE, Shikhaliyeva I, Gumusderelioglu M (2019) Boron mediated 2D and 3D cultures of adipose derived mesenchymal stem cells. Cytotechnology 71:611–622
25. Bolgen N, Vargel I, Korkusuz P, Guzel E, Plieva F, Galaev I, Matiasson B, Piskin E (2009) Tissue responses to novel tissue engineering biodegradable cryogel scaffolds: an animal model. J Biomed Mater Res A 91:60–68
26. Preethi Soundarya S, Haritha Menon A, Viji Chandran S, Selvamurugan N (2018) Bone tissue engineering: scaffold preparation using chitosan and other biomaterials with different design and fabrication techniques. Int J Biol Macromol 119:1228–1239
27. Mishra R, Bishop T, Valerio IL, Fisher JP, Dean D (2016) The potential impact of bone tissue engineering in the clinic. Regen Med 11:571–587
28. Roddy E, DeBaun MR, Daoud-Gray A, Yang YP, Gardner MJ (2018) Treatment of critical-sized bone defects: clinical and tissue engineering perspectives. Eur J Orthop Surg Traumatol 28:351–362
29. Panetta NJ, Gupta DM, Longaker MT (2009) Bone tissue engineering scaffolds of today and tomorrow. J Craniofac Surg 20: 1531–1532
30. Calis M, Demirtas TT, Vatansever A, Irmak G, Sakarya AH, Atilla P, Ozgur F, Gumusderelioglu M (2017) A biomimetic alternative to synthetic hydroxyapatite: "boron-containing bone-like hydroxyapatite" precipitated from simulated body fluid. Ann Plast Surg 79: 304–311
31. Bakhshandeh B, Zarrintaj P, Oftadeh MO, Keramati F, Fouladiha H, Sohrabi-Jahromi S, Ziraksaz Z (2017) Tissue engineering; strategies, tissues, and biomaterials. Biotechnol Genet Eng Rev 33:144–172
32. Paschos NK, Brown WE, Eswaramoorthy R, Hu JC, Athanasiou KA (2015) Advances in tissue engineering through stem cell-based co-culture. J Tissue Eng Regen Med 9:488–503
33. Zuk PA, Zhu M, Ashjian P, De Ugarte DA, Huang JI, Mizuno H, Alfonso ZC, Fraser JK, Benhaim P, Hedrick MH (2002) Human adipose tissue is a source of multipotent stem cells. Mol Biol Cell 13:4279–4295
34. Zuk PA, Zhu M, Mizuno H, Huang J, Futrell JW, Katz AJ, Benhaim P, Lorenz HP, Hedrick MH (2001) Multilineage cells from human adipose tissue: implications for cell-based therapies. Tissue Eng 7:211–228
35. Calis M, Demirtas TT, Atilla P, Tatar I, Ersoy O, Irmak G, Celik HH, Cakar AN, Gumusderelioglu M, Ozgur F (2014) Estrogen as a novel agent for induction of adipose-derived mesenchymal stem cells for osteogenic differentiation: in vivo bone tissue-engineering study. Plast Reconstr Surg 133:499e–510e
36. Mester E, Nagylucskay S, Tisza S, Mester A (1978) Stimulation of wound healing by means of laser rays. Part III–investigation of the effect on immune competent cells. Acta Chir Acad Sci Hung 19: 163–170
37. Mester E, Spiry T, Szende B (1973) Effect of laser rays on wound healing. Bull Soc Int Chir 32:169–173
38. Aimbire F, Albertini R, Pacheco MT, Castro-Faria-Neto HC, Leonardo PS, Iversen VV, Lopes-Martins RA, Bjordal JM (2006) Low-level laser therapy induces dose-dependent reduction of TNFalpha levels in acute inflammation. Photomed Laser Surg 24: 33–37
39. Lubart R, Lavi R, Friedmann H, Rochkind S (2006) Photochemistry and photobiology of light absorption by living cells. Photomed Laser Surg 24:179–185
40. Karu T (1999) Primary and secondary mechanisms of action of visible to near-IR radiation on cells. J Photochem Photobiol B 49: 1–17
41. Medrado AP, Soares AP, Santos ET, Reis SR, Andrade ZA (2008) Influence of laser photobiomodulation upon connective tissue remodeling during wound healing. J Photochem Photobiol B 92:144–152
42. Brightman LA, Brauer JA, Anolik R, Weiss ET, Karen J, Chapas A, Hale E, Bernstein L, Geronemus RG (2011) Reduction of thickened flap using fractional carbon dioxide laser. Lasers Surg Med 43:873–874
43. Abinaya B, Prasith TP, Ashwin B, Viji Chandran S, Selvamurugan N (2019) Chitosan in surface modification for bone tissue engineering applications. Biotechnol J:e1900171
44. Hollinger JO, Schmitt JM, Buck DC, Shannon R, Joh SP, Zegzula HD, Wozney J (1998) Recombinant human bone morphogenetic protein-2 and collagen for bone regeneration. J Biomed Mater Res 43:356–364
45. Nichol JW, Koshy ST, Bae H, Hwang CM, Yamanlar S, Khademhosseini A (2010) Cell-laden microengineered gelatin methacrylate hydrogels. Biomaterials 31:5536–5544
46. Klotz BJ, Gawlitta D, Rosenberg A, Malda J, Melchels FPW (2016) Gelatin-methacryloyl hydrogels: Towards biofabrication-based tissue repair. Trends Biotechnol 34:394–407
47. Djagny VB, Wang Z, Xu S (2001) Gelatin: a valuable protein for food and pharmaceutical industries: review. Crit Rev Food Sci Nutr 41:481–492
48. Lai JY, Li YT (2010) Functional assessment of cross-linked porous gelatin hydrogels for bioengineered cell sheet carriers. Biomacromolecules 11:1387–1397
49. Si Z, Wang X, Sun C, Kang Y, Xu J, Wang X, Hui Y (2019) Adipose-derived stem cells: sources, potency, and implications for regenerative therapies. Biomed Pharmacother 114:108765
50. Fraser J, Wulur I, Alfonso Z, Zhu M, Wheeler E (2007) Differences in stem and progenitor cell yield in different subcutaneous adipose tissue depots. Cytotherapy 9:459–467
51. Barbatelli G, Murano I, Madsen L, Hao Q, Jimenez M, Kristiansen K, Giacobino JP, De Matteis R, Cinti S (2010) The emergence of cold-induced brown adipocytes in mouse white fat depots is determined predominantly by white to brown adipocyte transdifferentiation. Am J Physiol Endocrinol Metab 298:E1244–E1253
52. Baer PC, Koch B, Hickmann E, Schubert R, Cinatl J Jr, Hauser IA, Geiger H (2019) Isolation, characterization, differentiation and immunomodulatory capacity of mesenchymal stromal/stem cells from human perirenal adipose tissue. Cells 2019 Oct 29 8(11):0